International Journal of Mechanical, Industrial and Aerospace Sciences
ISSN: 2517-9950
Vol:4, No:5, 2010

Effects of temperature-dependent material properties on stress and temperature in cracked metal plate under electric current load

Thomas Jin-Chee Liu

***Abstract*—**Using the finite element analyses, this paper discusses the effects of temperature-dependent material properties on the stress and temperature fields in a cracked metal plate under the electric current load. The practical and complicated results are obtained when the temperature-dependent material properties are adopted in the analysis. If the simplified (temperature-independent) material properties are used, incorrect results will be obtained.

***Keywords*—**Joule heating, temperature-dependent, crack tip, finite element.

I. Introduction

DUE to the electric current load and Joule heating effect, the electric current density concentration at the crack tip induces a local high temperature area in a cracked metal plate. However, a local melting region around the crack tip may be produced when the electrical energy is applied enough.

Under high current density and temperature at the crack tip, the heat source may cause a melting crack tip such as a heat affected zone (HAZ). During the cooling process, the melting material returns to the solid state and the crack sharp tip may disappear. A circular or elliptical hole, like a drilled hole, can be produced at the original crack tip after cooling [1-3]. Furthermore, the hole can arrest the crack propagation. In addition, the compressive stresses around the crack tip due to the temperature difference also retard the crack growth [1,2]. Like a crack repair method, this crack-arrest technique as shown in Fig. 1 can be used to control the crack growth in the aircraft and structural engineering [1].

In early studies, it has been reported that the Joule heating effect can induce local compressive thermoelastic stresses and melting area at the crack tip arresting crack propagation [4,5]. Using analytical methods, the cracked conducting plate and shell under an electric current have been studied in [6,7]. The most Joule heating concentration was shown to occur around the crack tip. Also, the Joule heating density became highly oscillatory along the crack due to thermal buckling under specific conditions [6,7]. In addition, the finite element analyses and results of electric current-induced stresses at the crack tip in conductors can be found in [8]. The electromagnetic and thermal stresses were obtained by the coupled-field analyses in their paper.

Experiments have reported that crack tips can melt under high electric current loading and a crack tip hole occurs after the subsequent cooling process [2,3,9]. From metallographic results in [3], it has been found that a typical fine phase transformation microstructure can be obtained in the crack tip region as a result of rapid heating and cooling. The intensity, ductility and wear capacity around the crack tip were promoted [3].

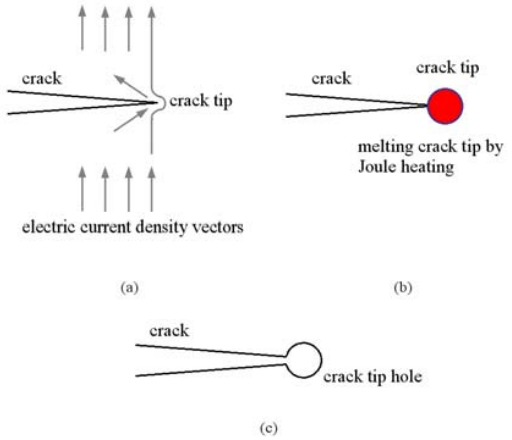

Fig. 1 Crack-arrest technique [1]

Based on the previous study in [1], this paper discusses the effects of temperature-dependent material properties on the stress and temperature fields in a cracked metal plate under the electric current load. The finite element software ANSYS [10] is adopted for solving the problems. The direct current (DC), alternating current (AC) and crack contact conditions will also be considered. The stress field and crack tip temperature will be obtained for estimating the crack tip behaviors.

II. Problem Description

The configuration of the problem is illustrated in Fig. 2. A metal plate with a central crack is subjected to a remote stress σ_0 and an electric current I_0. This thin plate is made of mild steel with dimensions $2W \times 2L$ and small thickness e. The crack length is $2a$.

Thomas Jin-Chee Liu is with the Department of Mechanical Engineering, Ming Chi University of Technology, Taishan, Taipei County 243, TAIWAN (corresponding author to provide phone: 886-2-29089899 ext 4569; e-mail: jinchee@mail.mcut.edu.tw).

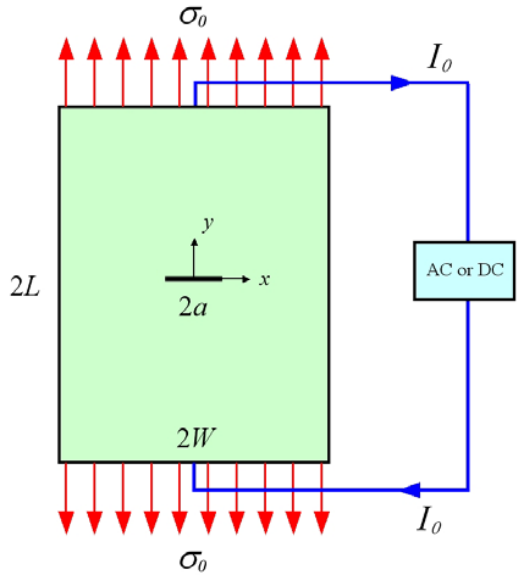

Fig. 2 Configuration of the problem

The thermo-electro-structural coupled-field problem in Fig. 2 will be solved by the finite element method. The plane stress, two-dimensional thermo-electric conditions, linear elastic and isotropic properties are assumed. The phase change effect is ignored [1].

To simulate more practical conditions, the temperature-dependent material properties in Table I [11] should be adopted in the analysis. The use of the temperature-independent material properties may lead to incorrect results. This issue will be discussed in this paper.

TABLE I
TEMPERATURE-DEPENDENT PROPERTIES OF MILD STEEL [11]

Temperature (°C)	Young's modulus E (GPa)	Coefficient of thermal expansion α (1/°C)	Thermal conductivity k (W/ m-°C)	Specific heat C_p (J/ kg-°C)	Resistivity ρ (Ω-m)
21	206.8	10.98×10^{-6}	64.60	444	0.14224×10^{-6}
93	196.5	11.52×10^{-6}	63.15	452.38	0.18644×10^{-6}
204	194.4	12.24×10^{-6}	55.24	511.02	0.26670×10^{-6}
315.5	186	12.96×10^{-6}	49.87	561.29	0.37592×10^{-6}
426.7	169	13.50×10^{-6}	44.79	611.55	0.49530×10^{-6}
537.8	117	14.04×10^{-6}	39.71	661.81	0.64770×10^{-6}
648.9	55	14.58×10^{-6}	34.86	762.34	0.81788×10^{-6}
760	6.9	14.05×10^{-6}	30.46	1005.3	1.0109×10^{-6}
871	–	13.05×10^{-6}	28.37	1005.3	1.1151×10^{-6}
982	–	–	27.62	1005.3	1.1582×10^{-6}
1093	–	–	28.52	1189.6	1.1786×10^{-6}
1204	–	–	–	1189.6	1.2090×10^{-6}

Poisson's ratio ν= 0.3, density β= 7861.2 kg/m^3, melting point = 1521 ºC.

The external current I_0 can be AC or DC. When the AC is used, the function of $I_0(t)$ is:

$$I_0(t) = I_A \sin(2\pi f t) \tag{1}$$

where t, I_A and f are the time, amplitude and frequency, respectively. A constant value of I_0 is used to simulate the DC.

Under thermo-electric Joule heating, the current-induced thermoelastic problem is transient. Contact conditions between both crack surfaces are considered in this study. The electric current and heat flow can pass through the crack surfaces when the crack contact occurs.

From the results of finite element analyses, the stress field and crack tip temperature will be obtained in order to estimate the crack tip behavior.

III. PRINCIPLES OF ANALYSES

A. Electric Current Analysis [12]:

$$\mathbf{E} = -\nabla\phi \ , \ \mathbf{J} = \frac{1}{\rho}\mathbf{E} \ , \ \nabla\cdot\mathbf{J} = 0 \tag{2}$$

where $\mathbf{E}$, $\mathbf{J}$, ϕ and ρ are the electric field, electric current density, electric potential and resistivity, respectively.

B. Thermal Analysis [12,13]:

$$\mathbf{q}'' = -k\nabla T \ , \ k\nabla^2 T + \dot{q} = \beta C_p \frac{\partial T}{\partial t} \ , \ \dot{q} = \rho|\mathbf{J}|^2 \tag{3}$$

where $\mathbf{q}''$, k, T, $\dot{q}$, β, C_p and t are the heat flux, thermal conductivity, temperature, heat generation of Joule heating, mass density, specific heat and time, respectively.

C. Thermoelastic Analysis [14]:

$$\sigma_{ji,j} + X_i = \beta\,\ddot{u}_i \ , \ i,j=x,y,z \tag{4}$$

$$\varepsilon_{ij} = \frac{1}{2}(u_{i,j} + u_{j,i}) \ , \ i,j=x,y,z \tag{5}$$

$$\varepsilon_{ij} = \frac{1}{E}\left[(1+\nu)\sigma_{ij} - (\nu I_1 - E\alpha\Delta T)\delta_{ij}\right] \ , \ i,j=x,y,z \tag{6}$$

where σ_{ij}, ε_{ij}, X_i, u_i, $\ddot{u}_i$, E, ν, I_1, ΔT and δ_{ij} are the stress, strain, body force, displacement, acceleration, Young's modulus, Poisson's ratio, stress invariant ($I_1=\sigma_{xx}+\sigma_{yy}+\sigma_{zz}$), temperature difference ($\Delta T = T - T_0$ where T_0 is the reference temperature) and Kronecker delta, respectively.

D. Coupled-Field Analysis [10]:

In this study, the finite element equations of the thermo-electro-structural coupled-field analysis are as follows [10]:

$$\begin{bmatrix} \mathbf{M} & 0 & 0 \\ 0 & 0 & 0 \\ 0 & 0 & 0 \end{bmatrix} \begin{bmatrix} \ddot{\mathbf{U}} \\ \ddot{\mathbf{T}} \\ \ddot{\mathbf{V}} \end{bmatrix} + \begin{bmatrix} \mathbf{C} & 0 & 0 \\ \mathbf{C}^{tu} & \mathbf{C}^{t} & 0 \\ 0 & 0 & 0 \end{bmatrix} \begin{bmatrix} \dot{\mathbf{U}} \\ \dot{\mathbf{T}} \\ \dot{\mathbf{V}} \end{bmatrix} + \begin{bmatrix} \mathbf{K} & \mathbf{K}^{ut} & 0 \\ 0 & \mathbf{K}^{t} & 0 \\ 0 & 0 & \mathbf{K}^{v} \end{bmatrix} \begin{bmatrix} \mathbf{U} \\ \mathbf{T} \\ \mathbf{V} \end{bmatrix} = \begin{bmatrix} \mathbf{F} \\ \mathbf{Q} \\ \mathbf{I} \end{bmatrix} \tag{7}$$

where **U**, **T**, **V**, **F**, **Q** and **I** are the vector forms of the displacement, temperature, electric potential, force, heat flow rate and electric current, respectively. The material constant matrices **M**, **C**, $\mathbf{C}^{t}$, $\mathbf{C}^{tu}$, **K**, $\mathbf{K}^{t}$, $\mathbf{K}^{ut}$ and $\mathbf{K}^{v}$ are the structural mass, structural damping, thermal specific heat, thermoelastic damping, structural stiffness, thermal conductivity, thermoelastic stiffness and electric conductivity, respectively. The coupled heat flow matrix **Q** contains the effects of the thermal loading and electrical Joule heating. $\mathbf{C}^{tu}$ and $\mathbf{K}^{ut}$ are thermoelastic coupled terms. Eq. (7) is a directly coupled nonlinear equation which is solved using the Newton-Raphson iterative method. Eqs. (2)–(7) will be solved using the finite element software ANSYS [10].

E. Boundary Conditions and Initial Conditions:

$$J(x,-L,t)=J_0(t)\ ,\ \ \phi(x,L,t)=0\ ,\ \ |x|\le W \tag{8}$$

$$\sigma_{yy}(x,L,t)=\sigma_{yy}(x,-L,t)=\sigma_0\ \ ,\ \ |x|\le W \tag{9}$$

$$T(x,y,0)=T_0=21°C \tag{10}$$

$$u_i(x,y,0)=\dot{u}_i(x,y,0)=\ddot{u}_i(x,y,0)=0 \tag{11}$$

where $J_0(t)=I_0(t)/(2We)$. As the time span is relatively short in the transient thermal analysis, all surfaces of the plate are assumed to undergo adiabatic processes [1,8].

On the crack surfaces ($-a<x<a$, $y=0$), the electrical-thermal-mechanical contact conditions with contact parameters will be considered in the numerical simulations. The following equations may describe the electrical and thermal contact conditions [10,15]：

$$J=\eta_{cel}(\phi_1-\phi_2) \tag{12}$$

$$q''=\eta_{cth}(T_1-T_2) \tag{13}$$

where η_{cel} and η_{cth} are respectively the electrical conductance and thermal conductance of the contact surfaces. The terms $(\phi_1-\phi_2)$ and (T_1-T_2) are respectively the electric potential difference and temperature difference between both contact surfaces.

IV. Finite Element Model

The finite element model of the previous study [1] is also adopted in this paper. The accuracy of the mesh has been validated in [1]. Fig. 3 shows the finite element mesh of ANSYS with $W=L=0.05$ m and $a=0.01$ m. Due to the symmetry of the problem, only a half plate of Fig. 2 is analyzed and the symmetric conditions are applied on the model. The plate is modeled by ANSYS element type: PLANE223, i.e. the 8-node isoparametric plane element with the thermo-electro-structural coupled-field analysis. The plane stress option is used due to the thin thickness. The nodal degrees-of-freedom of PLANE223 are u_x, u_y, T, and ϕ. In Fig. 3, the model has 1822 elements and 5353 nodes. The quarter-point elements (QPE) [16] are used for modeling the $r^{-1/2}$ singularity at the crack tip. In this study, the length of QPE along the crack denotes b and the ratio $b/a=1/40$.

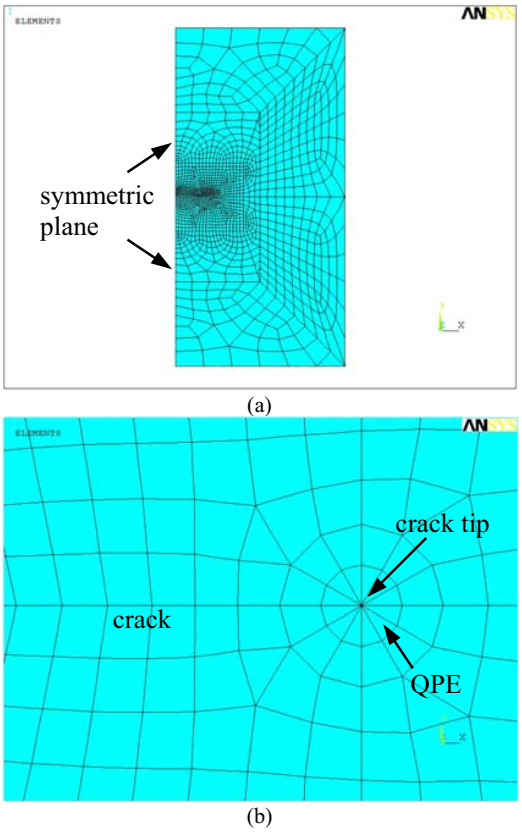

Fig. 3 Finite element model (a)global view (b)local view

V. Results and Discussions

A. Electric Current Density and Temperature Field near Crack Tip

In this case, the following dimensions of the plate are considered: $W=L=0.05$ m, $a=0.01$ m and $e=0.001$ m. The DC $I_0=25000$ A and remote stress $\sigma_0=10$ MPa are used. Also, the temperature-dependent material data in Table I are adopted in the analysis.

As a result in Fig. 4, it shows the electric current density vectors near the crack tip at $t=0.050169$ s. Due to the opening condition of the crack, the vectors can not pass through the crack surfaces. It is noted that there is a field concentration at the crack tip. Similar to the elastic stress field, the electric current density also has the $r^{-1/2}$ singularity at the crack tip [1,2,8].

In Fig. 5, the electric current density J_y in the y-direction performs the singular phenomenon near the crack tip ($x=0.01$ m). This curve performs irregular shape due to the temperature-dependent material data.

At the crack tip, the Joule heating effect causes a high temperature area. Fig. 6 shows the temperature contour in the

plate at t=0.050169 s. In Fig. 6(b), it demonstrates the melting crack tip (red color area) when enough electrical energy is provided. In Fig. 7, the highest temperature occurs at the crack tip (x=0.01 m).

When the electrical energy is applied on the metal plate, the temperature field increases with time. Fig. 8 depicts the history of the temperature change.

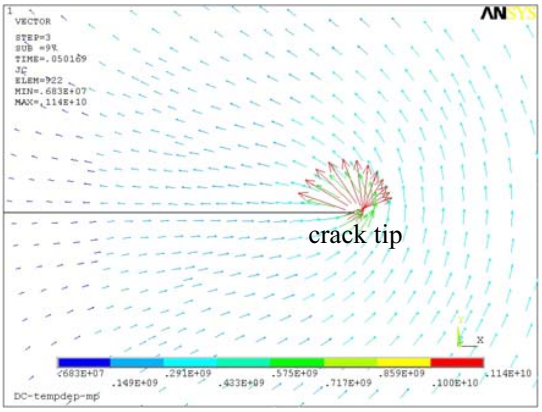

Fig. 4 Electric current density vectors (units: A/m^2)

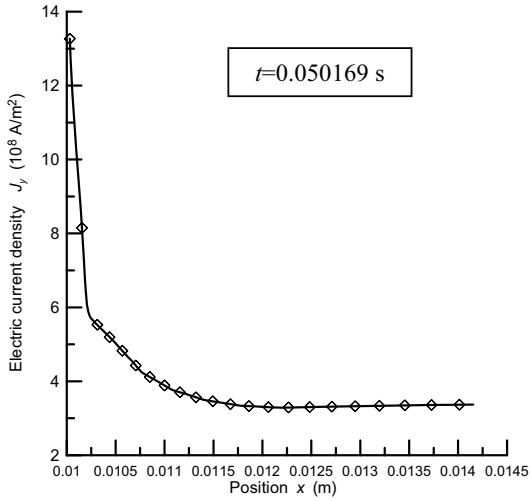

Fig. 5 Electric current density J_y versus position

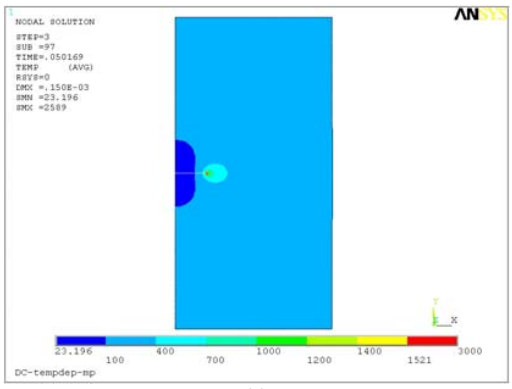

(a)

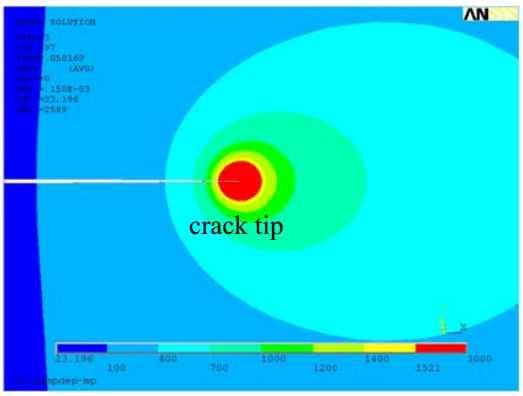

(b)

Fig. 6 Temperature contour (a)global view (b)local view

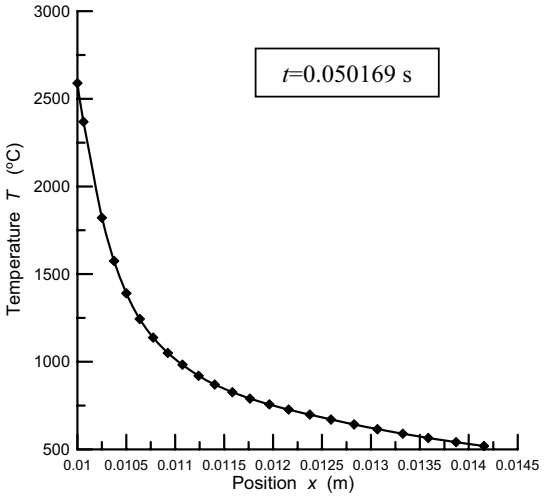

Fig. 7 Temperature versus position

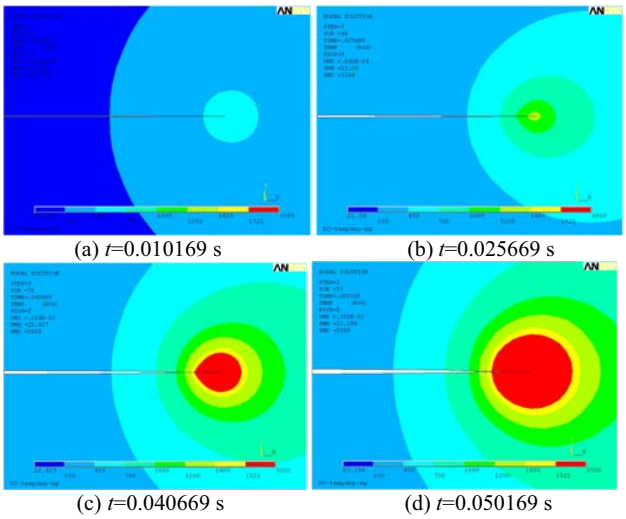

(a) t=0.010169 s (b) t=0.025669 s

(c) t=0.040669 s (d) t=0.050169 s

Fig. 8 Temperature contours at different times

B. Crack Tip Temperature

In this section, the DC or AC is used. The numerical results from the temperature-dependent material data are compared with those from the temperature-independent material data. The later one uses the material constants at 21°C in TABLE I.

In Fig. 9, it shows the effects of temperature-dependent material properties on the crack tip temperature under I_0=22000 A. When the temperature-dependent material data are used, the crack tip can melt after t=0.045 s. On the contrary, the crack tip cannot melt if the temperature-independent material data are used.

In addition, Fig. 10 shows similar results under the AC load which is $I_0(t) = 22000\sin(120\pi t)$ A. The frequency of AC is 60 Hz.

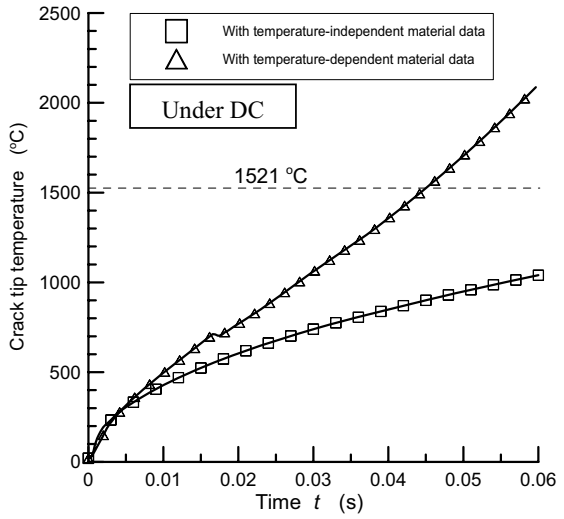

Fig. 9 Crack tip temperature versus time (melting point = 1521 ºC)

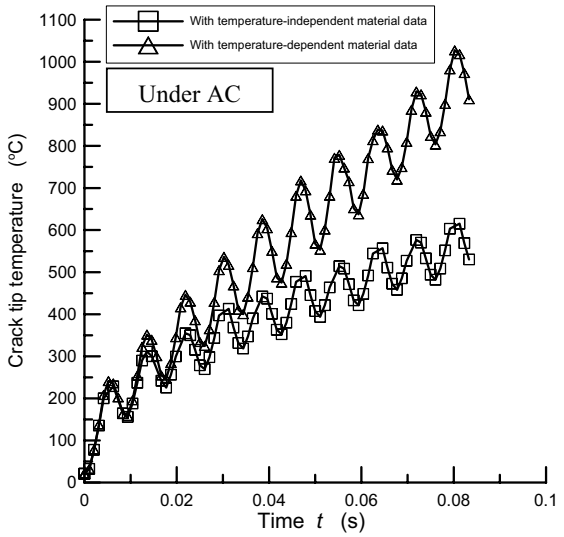

Fig. 10 Crack tip temperature versus time

All data in TABLE I should be adopted in the analyses to obtain correct results. If the simplified (temperature-independent) material data are used, the temperatures are incorrect.

C. Stress Field

In Fig. 11, it shows the effects of temperature-dependent material properties on the stress σ_y under I_0=22000 A. The case with simplified (temperature-independent) material data performs larger compressive stress near the crack tip (x=0.01 m). It can be seen that the compressive stresses occur in the front of the crack tip. It will retard the crack growth.

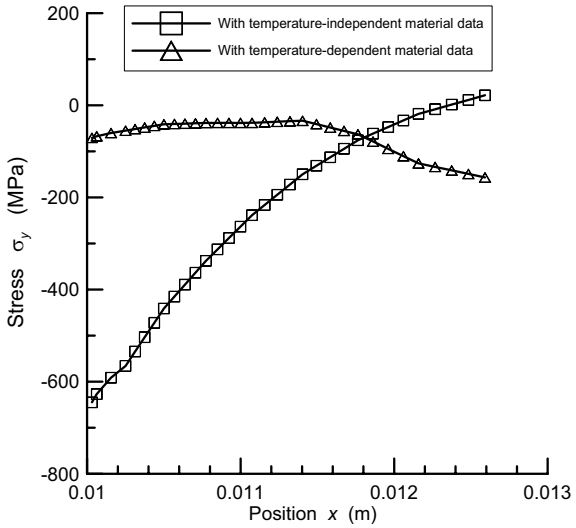

Fig. 11 Stress σ_y versus time (t=0.06 s)

VI. Conclusion

Using the finite element method, this paper has discussed the effects of temperature-dependent material properties on the stress and temperature fields in a cracked metal plate under the electric current load. At the crack tip, the Joule heating effect causes a high temperature area or melted region. The practical and complicated results are obtained when the temperature-dependent material properties are adopted in the analysis. If the simplified (temperature-independent) material properties are used, incorrect results will be obtained.

Acknowledgment

The author is grateful to the National Science Council in Taiwan for the financial support under contract number NSC 97-2221-E-131-012.

References

[1] T.J.C. Liu, "Thermo-electro-structural coupled analyses of crack arrest by Joule heating," *Theor. Appl. Fract. Mech.*, vol. 49, pp. 171–184, 2008.

[2] X.Z. Bai, Z.G. Tian and J. Zheng, *Thermo-Electric Effects in Fracture Mechanics*. Beijing, China: National Defense Industry Press, 2009. (in Chinese)

[3] Y.M. Fu, X.Z. Bai, G.Y. Qiao, Y.D. Hu and J.Y. Luan, "Technique for producing crack arrest by electromagnetic heating," *Mater. Sci. Tech.*, vol. 17, pp.1653–1656, 2001.
[4] B.A. Kudryavtsev, V.Z. Parton and B.D. Rubinskii, "Electromagnetic and thermoelastic fields in a conducting plate with a cut of finite length," *Solids. Mech.*, vol. 17, pp. 110–118, 1982.
[5] V.Z. Parton and B.A. Kudryavtsev, *Electromagnetoelasticity*. New York: Gordon and Breach, 1988.
[6] D. Hasanyan, L. Librescu, Z. Qin and R.D. Young, "Thermoelastic cracked plates carrying nonstationary electrical current," *J. Therm. Stress*, vol. 28, pp. 729–745, 2005.
[7] Z. Qin, L. Librescu and D. Hasanyan, "Joule heating and its implications on crack detection/arrest in electrically conductive circular cylindrical shells," *J. Therm. Stress*, vol. 30, pp. 623−637, 2007.
[8] G.X. Cai and F.G. Yuan, "Electric current-induced stresses at the crack tip in conductors," *Int. J. Fract.*, vol. 96, 279–301, 1999.
[9] Y.M. Fu, X.Z. Bai and L.J. Zheng, "Numerical simulation and experimental research on crack arresting using electromagnetic heat effects," *Int. J. Nonlin. Sci. Num.*, vol. 2, pp. 375-378, 2001.
[10] *ANSYS HTML Online Documentation*. USA: SAS IP, Inc., 2005.
[11] C.L. Tsai, W.L. Dai, D.W. Dickinson and J.C. Papritan, "Analysis and development of a real-time control methodology in resistance spot welding," *Weld. J.*, vol. 70, pp. s339–351, 1991.
[12] D.K. Cheng, *Field and Wave Electromagnetics*. MA: Addison-Wesley, 1983.
[13] F.P. Incropera and D.P. DeWitt, *Fundamentals of Heat and Mass Transfer*. Fifth ed., USA: John Wiley & Sons, 2002.
[14] A.P. Boresi and K.P. Chong, *Elasticity in Engineering Mechanics*. Second ed., New York : John Wiley & Sons, 2000.
[15] X. Sun and P. Dong, "Analysis of aluminum resistance spot welding processes using coupled finite element procedures," *Weld. J.*, vol. 79, pp. s215-s221, 2000.
[16] R.S. Barsoum, "On the use of isoparametric finite elements in linear fracture mechanics," *Int. J. Numer. Meth. Eng.*, vol. 10, pp. 25-37, 1976.

Thomas Jin-Chee Liu is an Associate Professor in Department of Mechanical Engineering, Ming Chi University of Technology, Taiwan. He received the Ph.D. degree in Mechanical Engineering from National Cheng Kung University in 2005. His research interests are fracture mechanics, solid mechanics, finite element analyses, computer-aided engineering (CAE), crack repair, piezoelectric problems, magneto-electro-elastic problems, biomechanics and vehicle structures.